Equilibrium and kinetic study of adsorption of diazinon from aqueous solutions by nano-polypropylene-titanium dioxide: Optimization of adsorption based on response surface methodology (RSM) and central composite design (CCD)

Asma Barazandeh[*], Hamzeh Ali Jamali[*], and Hamid Karyab[**,†]

*Department of Environmental Health Engineering, School of Health, Qazvin University of Medical Sciences, Qazvin, Iran
**Social Determinants of Health Research Center, Qazvin University of Medical Sciences, Qazvin, Iran

Abstract−This study evaluated the applicability of the adsorption of a widely used organophosphorous pesticide named diazinon, from aqueous using a new composite consisting of nan-TiO_2 and polypropylene (Nano-PP/TiO_2). The Nano-PP/TiO_2 was prepared by wet heat with submerging in an ultrasonic chamber. Extraction and analysis of diazinon were accomplished with dispersive liquid-liquid-microextraction and gas chromatography. By using FTIR, SEM, TEM, and BET technologies, specifications of Nano-PP/TiO_2 structure were determined. Adsorption equilibrium and kinetics of diazinon were investigated in a batch reactor and the effects of adsorbent dose, contact time, and initial concentrations of diazinon were assessed. It was found that the two-parameter models arranged the data better than the three-parameter, and the equilibrium data was represented properly by the Langmuir. Additionally, it was identified that adsorption followed the pseudo-second-order kinetic model. To optimize the conditions for maximum adsorption of diazinon, response surface methodology was implemented the effects of factors on the adsorption efficiency were surveyed. The values of optimal initial diazinon concentration, contact time, and mass of Nano-PP/TiO_2 were obtained at 10 mg L^{-1}, 32.2 min, and 2.25 g L^{-1}, respectively. Based on the results, the Nano-PP/TiO_2 can be used as an effective and efficient adsorbent for the removal of diazinon from aqueous.

Keywords: Diazinon, Nano-composite, Water, Wastewater, Adsorption

INTRODUCTION

Water supplies are a fundamental right and a primary requirement for humankind [1]. Insufficient access to safe and adequate water leads to the spread of disease, causing critical public health problems, such as infectious diseases and gastrointestinal cancer [2,3]. In present times, contamination is one of the most important problems increasing gradually in the surrounding environment. Pollution of aquatic environments by organic pesticides is one of the most common types of environmental pollution that is often caused by human activities [4].

These pesticides come in a variety of ways, including the discharge of sewage, direct washing of pesticides, surface runoff, agricultural drainage, erosion, and regional application [5-7]. Diazinon, an organophosphorus pesticide, is widely used in agricultural activities and is identified as a pollutant in many water resources [8]. The World Health Organization (WHO) confirmed that its toxicity was 350 ng L^{-1} for aquatic and about 90-444 mg Kg^{-1} of body weight for humans [9].

Many methods, such as ozonation [10], photocatalytic degradation [11], electrocoagulation process using aluminum electrodes [12], and adsorption methods [13,14] have been developed to remove diazinon from water resources and wastewater. Among them, due to technological, environmental, and economic aspects, the application of the adsorption process in the removal of diazinon is very popular and the most attractive option [15-17].

Polypropylene (PP) is a semi-crystalline polymer of the thermoplastic polyolefin polymer family. In accordance with good processing capability and chemical properties, PP is used as primary polymer in technical applications for water treatment [18,19]. Additionally, titanium dioxide is an inexpensive photo-catalyst that kills the bacteria due to its high reactivity and improves the performance of PP when used in combination. So recently, titanium dioxide (TiO_2) in a mixture with PP has attracted much attention; however, this depends on the mixing patterns, particle size, and carbon content of the TiO_2 nano-powders [20].

Karyab et al. showed that polypropylene and titanium dioxide nanocomposite can be used effectively to remove total organic carbon (TOC) from water. Also, in another study, they examined and reported its efficiency in removing lightweight petroleum hydrocarbons from contaminated water resources [21]. As mentioned, the potential of Nano-PP/TiO_2 had been proved in the adsorption of total organic carbon (TOC) from water resources. However, we could not find any evidence related to removing diazinon by Nano-PP/TiO_2. So the purpose of this study was to evaluate the adsorption potential of diazinon organophosphate pesticides by Nano-

PP/TiO$_2$, as an inexpensive and affordable adsorbent.

METHODS

1. Materials

A primary and effective study was done recently at the School of Health Sciences in Qazvin University of Medical Science, Iran. This study evaluated the adsorption of diazinon on polypropylene/titanium dioxide nanocomposite which was done in a batch reactor. A 1,000 mg L^{-1} stock solution of diazinon was prepared by using methanol. Methanol and diazinon were purchased from SIGMA-ALDRICH. The PP fibers with a density of 0.91 g cm^{-3}, a length of 0.01 m, a diameter of 330 micrometers were prepared in Razi Institute, Iran. Nano-TiO$_2$ with a diameter of 20 nm, a bulk density of 0.46 g mL^{-1}, and a surface area of 10 to 45 m^2 g^{-1} with a purity of >99% was purchased from NANOSANY, Iran, which contained anatase and rutile by volume of 80% and 20%, respectively.

2. Nano-composite Synthesis

PP/TiO$_2$ nanocomposite was synthesized in three phases: activation of PP fibers, coating of PP fiber with nano-TiO$_2$, and polishing. In the first and second phases, the PP fibers were activated and coated through wet heating for 90 min at 65 °C in a stainless steel chamber. Increasing contact time and temperature in PP activation was limited to prevent the fiber deformation. In various studies, activation of PP has been reported with different methods such as dry heat and plasma [22-24]. Subsequently, the activated fibers were coated with a nano-TiO$_2$ with a diameter of 20 nm. This coating phase was followed at 26 kHz and 100 W while keeping the temperature at 40 °C in a sonication chamber with 0.5, 1, and 2 mg L^{-1} concentrations of nano-TiO$_2$ solution. In previous studies, the feasibility of this method has already been reported [21]. Finally, the morphology of the fractured surfaces was examined by field emission scanning electron microscopy (FE-SEM). FTIR spectroscopy was employed to identify fiber-forming substances, using an EQUINOX55 FT-IR (Bruker Optics, Ettlingen, Germany). The pore size distribution and pore volume of PP/TiO$_2$ nanocomposite were assessed using multiple-point nitrogen adsorption through Brunauer-Emmett-Teller (BET) surface area analyzer (Belsorp Mini II, Japan). By using the amount of N$_2$ gas adsorbed at different partial pressures (p/p$_0$) and a single condensation point (p/p$_0$=0.98), BET analysis was applied. Particle distribution and titanium particle weight content in the PP/TiO$_2$ nanocomposite were analyzed with image analysis and EDS, using a Mira 3-XMU device equipped with an EDS micro-analyzer (TESCAN Corporation).

3. Extraction and Analysis

Diazinon was extracted by dispersive liquid-liquid microextraction (DLLME) method by using toluene solvent. For this purpose, 12 ml of sample was poured into a 12 ml vial that was specially designed to achieve this objective. Thereafter, 50 μls of toluene was injected into it, and the vial opening was covered with parafilm tape. The vial was then placed in an ultrasonic chamber for 10 minutes and centrifuged at 3,200 rpm for 3 minutes [4,25]. Finally, by utilizing the GC syringe, the vial supernatant was removed and injected into a gas chromatograph (Agilent 7890 FID, TCD capillary column) while keeping the helium gas flow at 1 ml min^{-1}, and the injector temperature at 250 °C. The injector was operated at 1-4

splits and the initial column temperature was regulated at 70 °C for 2 min. In a proper sequence, the temperature was increased at three steps: (a) at 25 °C min^{-1} up to 150 °C and maintained at that temperature for 2 min; (b) at 15 °C min^{-1} up to 220 °C and maintained at that temperature for 2 minutes, and (c) at 280 °C (8 °C min^{-1}) for 7 min. A calibration curve was prepared by stocking the solution including five concentrations of 100, 1,000, 5,000, 10,000, and 1,000,000 micrograms per liter (μg L^{-1}) for the quantification of sample analysis and injected into the gas chromatography with three replications. R^2 values calculated from trend lines were 0.9992.

Also, 21 spike samples at three concentrations including 5, 10,000, and 20,000 μg L^{-1} were assessed to control the quality of sample analysis. For the quality of control and analysis, the diazinon concentration was measured in triplicate at each phase using a GC analyzer. With a signal-to-noise ratio of three, the detection limit for diazinon ranged from 0.2 to 2 μg L^{-1}.

4. Batch Experiments and Validity Assessment

At the concentration of 1,000 mg L^{-1}, the stock solution of diazinon was prepared by methanol. By utilizing a rotary shaker, batch adsorption experiments were carried out at 100 rpm in 250-mL flasks. Diluted diazinon stock solutions were prepared at concentration of 5-2,000 μg L^{-1} by diluting the diazinon stock solution with distilled water at 23-25 °C ambient temperature and pH~7.5. Under similar conditions, batch kinetic and equilibrium experiments were conducted. Finally, by using Eqs. (1) to (3), the amount of adsorption at equilibrium, q$_e$ (mg g^{-1}), at time t, q$_t$ (mg g^{-1}), and the percent of adsorption (%) was computed where C$_0$, C$_e$, and C$_t$ are initial diazinon concentration (mg L^{-1}), equilibrium diazinon concentrations (mg L^{-1}), and diazinon concentration at time t (mg L^{-1}), respectively. V is the volume of the solution (L) and W is a dried form of Nano-PP/TiO$_2$ (g).

$$q_e = \frac{(C_0 - C_e)V}{W} \tag{1}$$

$$q_t = \frac{(C_0 - C_t)V}{W} \tag{2}$$

$$\%\,removal = \frac{(C_0 - C_e)}{C_i} \times 100 \tag{3}$$

RESULTS AND DISCUSSION

1. Characterization of the Nanocomposite

The surface structure of PP fibers before and after treatment with Nano-TiO$_2$ was analyzed using field-emission scanning electron microscopy (FE-SEM). FE-SEM micrographs provided useful resolution and permit repeated multi-site imaging of surfaces.

Fig. 1 shows the surface of the nanocomposite before and after treatment. As shown in Fig. 1(b), the surface of crude PP fiber was smooth and without any inconsistency after the treatment process. However, the surface of the nanocomposite was modifiable and appeared to bulge after synthesis. The FE-SEM micrographs showed that the dispersion of the Nano-TiO$_2$ particles was relatively good, and only a few aggregations exist. Also, MAP analyses were used to analyze the scratch surface and control the release of inhibitors. Fig. 1(c) displays the position of Nano-TiO$_2$ in the adsorbent. It
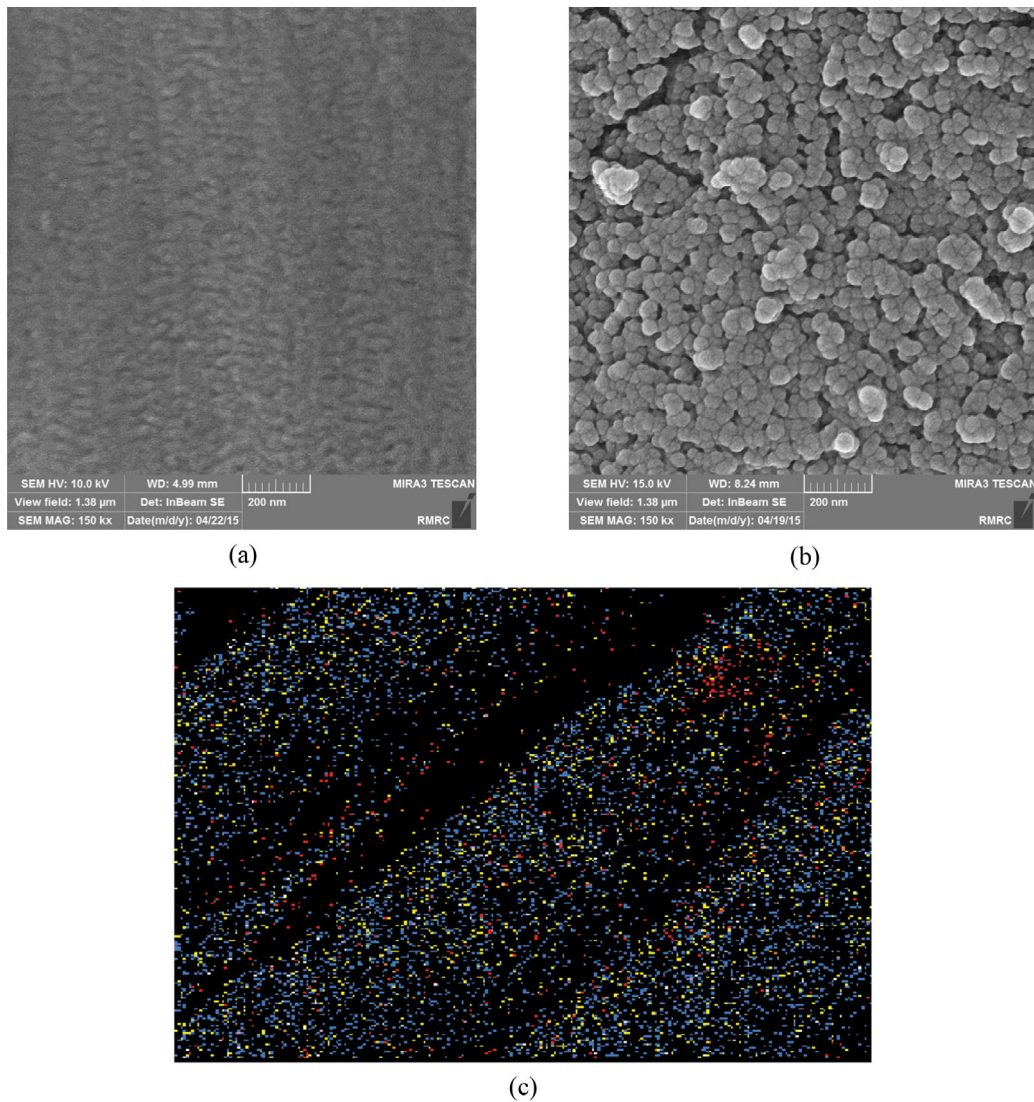
(a)

(b)

(c)

Fig. 1. Micrographs of scanning electron microscope. (a) Surface of PP fiber before treatment. (b) Surface of nanocomposite after treatment. (c) Position of Nano-TiO$_2$ (red points) in the sorbent.

reveals a change of appearance with the presence of Nano-TiO$_2$ particles (red points) adsorbed onto the surface after the treatment process. Fig. 2 shows the FT-IR spectra of the synthesized Nano-PP/
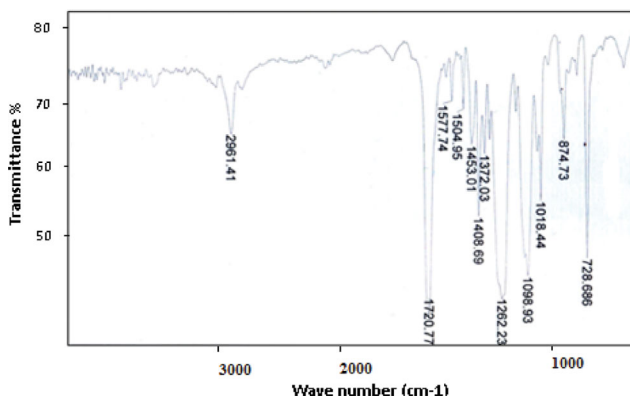

Fig. 2. FI-IR spectra of the synthesized Nano-PP/TiO$_2$.

TiO$_2$. Vibration peak at 1,570 to 700 cm^{-1} regions confirmed the presence of grafting on the composite surface. According to results of other studies, these peaks are thought to be formed due to the adsorption of titanium dioxide on the PP fibers [26,27].

As presented in Fig. 3, the energy-dispersive x-ray spectroscopy (EDX test) was performed to demonstrate the presence of titanium on the PP surface. This figure shows the EDX spectrum for the Nano-PP/TiO$_2$. The peaks corresponding to nitrogen, carbon, oxygen, and titanium are demonstrated in the spectrum, and the elemental analyses have shown that the composition of elements changed the after-treatment process. The weight of carbon, nitrogen, oxygen, and titanium after the treatment process in Nano-PP/TiO$_2$ was 69.5, 6.8, 22.5, and 3.7%, respectively.

Change of composition of elements can be attributed to the bonding of TiO$_2$ nanoparticles to the surface of the polypropylene after-treatment process. The aggregation of TiO$_2$ may be caused by surface reaction between the nanoparticles and polypropylene. Moreover, the property improvement of PP/TiO$_2$ nanocomposite
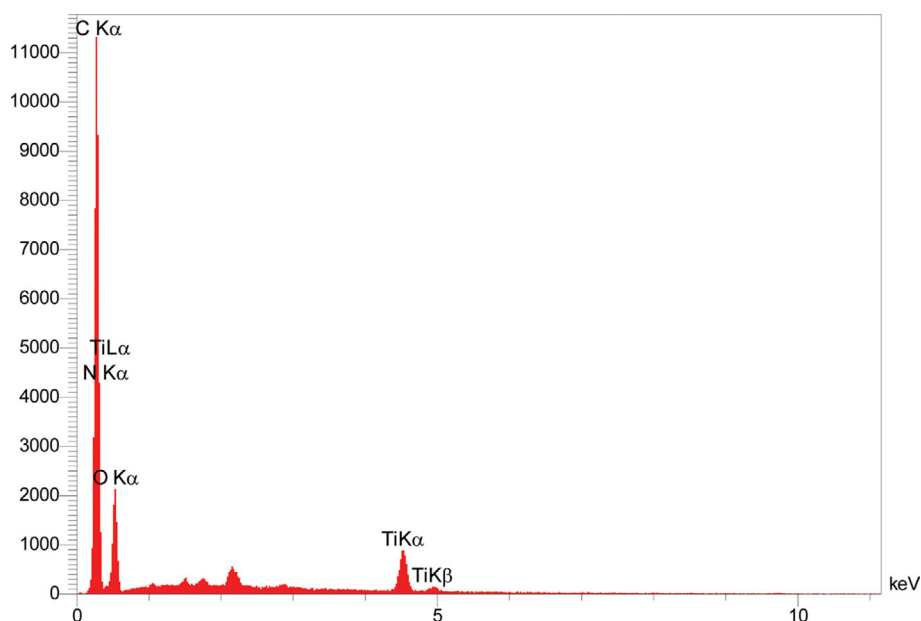
Fig. 3. EDX spectrum of synthesized Nano-PP/TiO$_2$ after treatment process.

may also be created due to the inherent stiffness and the dispersion qualities of TiO$_2$ [20].

The pore size distribution and pore volume of Nano-PP/TiO$_2$ were measured by using multiple points of nitrogen gas adsorption/desorption based on the Brunauer-Emmett-Teller (BET) analysis. The total pore volume of Nano-PP/TiO$_2$ was 2.06 cm^3 g^{-1} (p/p$_0$=0.98) with an average pore diameter of 2.48 nm and a surface area of 51.52 m^2 g^{-1}, which demonstrated that the prepared Nano-PP/TiO$_2$ had a high surface area and presents a high potential for adsorption of diazinon from aqueous.

2. Adsorption Isotherms

In this study, the capacity of Nano-PP/TiO$_2$ to absorb the diazinon is determined by measuring the equilibrium isotherms to describe

the interaction between diazinon and Nano-PP/TiO$_2$. The interaction between the amount of diazinon removed from samples at equilibrium by a unit of mass of Nano-PP/TiO$_2$ at constant temperature (23-25 ^{o}C at pH~7.5) was expressed with equilibrium data. This was fitted by three "two-parameter isotherms" including Freundlich, Langmuir, and Temkin, and Redlich-Peterson (three-parameter isotherm). Linear expression of these isotherm equations and the way to obtain the isotherm parameters are given in Table 1. Where C$_e$ denotes equilibrium concentration (mg L^{-1}), q$_e$ is expressed as the amount of diazinon adsorbed in equilibrium (mg g^{-1}), q$_m$ indicates the maximum amount of adsorption (mg g^{-1}), b is the adsorption equilibrium constant (L mg^{-1}), Kf denotes adsorption capacity (mg g^{-1}), n is adsorption intensity, and K$_T$ is the bind-

Table 1. Isotherms parameters by linear regression method for the sorption of diazinon by nano-polypropylene-titanium dioxide composite

Isotherms	Linear expression	Plot	Parameters in model	R^2	MPSD	HYBRID	Obtained parameters
Freundlich	$\ln q_e = \ln K_F + n^{-1} \ln C_e$	$\ln q_e$ vs. $\ln C_e$	K$_F$=exp(intercept) n=(slope)$^{-1}$	0.996	3.97	0.17	n=2.30 K$_F$=0.29 mg g^{-1}
Langmuir	Type(I) C_e/q_e =$(1/K_L q_m)+(C_e/q_m)$	(C_e/q_e) vs. C_e	q$_m$=(slope)$^{-1}$ K$_L$=slope/intercept	0.852	17.21	0.42	K$_L$=0.38 L mg^{-1}; q$_m$=1.24 mg g^{-1}
	Type(II) $1/q_e$ =$(1/K_L q_m C_e)+(1/q_m)$	$1/q_e$ vs. $1/C_e$	q$_m$=(intercept)$^{-1}$ K$_L$=intercept/slope	0.999	6.40	0.40	K$_L$=6.88 L mg^{-1}; q$_m$=0.908 mg g^{-1}
	Type(III) q_e =$q_m-(1/K_L)q_e/C_e$	q_e vs. q_e/C_e	q$_m$=intercept K$_L$=$-$(slope)$^{-1}$	0.817	7.10	0.43	K$_L$=6.32 L mg^{-1}; q$_m$=0.16 mg g^{-1}
	Type(IV) q_e/C_e =$K_L q_m - K_L q_e$	q_e/C_e vs. q_e	q$_m$=$-$(intercept/slope), K$_L$=$-$slope	0.817	8.43	0.51	K$_L$=5.17 L mg^{-1}; q$_m$=1.05 mg g^{-1}
Temkin	$q_e = q_m \ln K_T + q_m \ln C_e$	q_e vs. $\ln C_e$	q$_m$=slope, K$_T$=Exp(intercept/slope)	0.870	309.37	33.20	K$_T$=0.38 L mg^{-1}; q$_m$=1.24 mg g^{-1}
Redrish peterson	$\ln[(A_{RP}C_e/q_e)-1]=g$ $\ln C_e + \ln B_{RP}$	$\ln[(A_{RP}C_e/q_e)-1]$ vs. $\ln C_e$	g=slope, B$_{RP}$=Exp(intercept)	0.750	4.75	2.56	B$_{RP}$=1.074 (L mg^{-1})^g; A$_{RP}$=1.07 mg g^{-1} (L mg^{-1})

Table 2. Kinetic and isotherm models for adsobtion of diazinon on various adsorbents

Adsorbent	Consistent kinetics	Best fitted isotherm	Reference
Clay/graphene oxide/Fe_3O_4	Pseudo-second-order and Elovich	Langmuir-Freundlich	[14]
NH_4Cl-induced activated carbon	Pseudo-second-order	Langmuir	[29]
Alimentary industrial waste	Pseudo-second-order	Langmuir	[31]
Treated Bentonite with dilute H_2SO_4	Pseudo-second-order	Langmuir	[30]
Activated carbon and Loess soil	Pseudo-second-order	Freundlich	[15]
Magnetite nanoparticles coated with methoxy polyethylene glycol	---	Freundlich	[41]
Nano-TiO_2, Degussa P_{25}	--	first-order	[9]
Fe_3O_4/SiO_2 core/shell nanocrystals	Pseudo-second-order	Langmuir	[35]
Mg-Al and Zn-Al layered double hydroxides	intra-particle	Langmuir	[36]
Chitosan/carbon nanotube	Pseudo-second-order	Sips	[16]
Nano-PP/TiO_2 composite	Pseudo-second-order (type 1)	Langmuir (type 2)	Present study

ing constant representing the maximum binding energy (Temkin isotherm constant as L mg^{-1}). The applicable equation of the isotherm that described the adsorption process was analyzed by the coefficients of the correlation, suchlike R^2 values [28-30].

The derived outcomes revealed that the models of adsorption isotherm arranged the data in the sequence of Langmuir type 2, Freundlich, Temkin, Langmuir type 1, Langmuir type 3, Langmuir type 4, and Redlich-Peterson isotherm. The above sequence revealed that the equilibrium data is properly arranged by the two-parameter models rather than the three-parameter models. Similar results were presented in the process where diazinon was removed from contaminated water by adsorption onto NH_4Cl-induced activated carbon [29], and a pre-treated alimentary industrial waste [31].

The high regression coefficient showed that the Langmuir isotherm was the most suitable model to describe the adsorption of diazinon by Nano-PP/TiO_2 over the studied concentration ranges. Also, it was confirmed that some homogeneity in the Nano-PP/TiO_2 surface or inside the pores plays a role in the adsorption. It describes monolayer adsorption of diazinon onto Nano-PP/TiO_2 surface and the substances chemisorbed on the solid surface of adsorbent are hardly removed because of stronger forces at stake [32]. Moreover, it suggests that there is negligible interaction between the adsorbed molecules (diazinon) and adsorption sites in the Nano-PP/TiO_2 fibers [14,33].

In addition, the large K_L value (6.88 L mg^{-1}) implies a strong interaction with the diazinon/Nano-PP/TiO_2 composite. As presented in Eq. (4), the essential feature of the Langmuir isotherm can be expressed by a dimensionless separation factor (R_L) [31]:

$$R_L = 1/(1+K_L C_0) \tag{4}$$

where K_L and C_0 are Langmuir isotherm constant (L mg^{-1}) and initial diazinon concentrations, respectively. The value of the R_L's number divides the isotherm's type into unfavorable ($R_L > 1$), linear ($R_L = 1$), irreversible ($R_L = 0$), and favorable ($0 < R_L < 1$) values and, therefore, the separated factor (R_L) was increased from 0.007 to 0.996, and as a C_0 was increased from 0.005 to 20 mg L^{-1}.

In addition, the Redlich-Peterson equation was used as a connection between Langmuir and Freundlich isotherms. This model has three parameters and incorporates the advantageous signifi-

cance of both models. The Redlich-Peterson isotherm model can be applied to both a homogeneous and a heterogeneous system for a wide concentration range, and it combines the properties of the Freundlich and Langmuir isotherms in a single equation [34].

As presented in Table 2, similar results were obtained by other studies in adsorption of diazinon from water by various adsorbents including NH_4Cl-induced activated carbon [29], alimentary industrial waste [31], treated bentonite with dilute H_2SO_4 [30], Fe_3O_4/SiO_2 core/shell nanocrystals [35], and Mg-Al and Zn-Al layered double hydroxides [36]. However, a different finding was reported in using Nano-TiO_2, Degussa P25 fitted to first-order model [9], activated carbon and Loess soil fitted to Freundlich model [15], and chitosan/carbon nanotube fitted to Sips model [16].

The goodness-of-fit of isotherm equations was assessed by the Marquardt percent standard deviation (MPSD), and hybrid fractional error function (HYBRID) values, as presented in Eqs. (5) and (6), where q_i^{Exp} and q_i^{Cal} are experimental and calculated mass of diazinon adsorbed by PP/TiO_2 nanocomposite, N is the number of observations in the experimental isotherm, and P is the number of parameters in the regression model [28].

$$MPSD = 100 \sqrt{\left(\frac{1}{N-P}\sum_{i=1}^{N}\left(\frac{q_i^{Exp}-q_i^{Cal}}{q_i^{Exp}}\right)^2\right)} \tag{5}$$

$$HYBRID = \frac{100}{N-P}\sum_{i=1}^{N}\left[\frac{(q_i^{Exp}-q_i^{Cal})^2}{q_i^{Exp}}\right] \tag{6}$$

The values of the parameters and the coefficients of the correlation, MPSD, and HYBRID which were obtained in this study are listed in Table 1. MPSD and HYBRID values suggested that Freundlich isotherm provides a better model of the sorption system. It revealed that the difference between experimental data and anticipated values by Langmuir isotherm is very low and it is showing that this isotherm model is the best isotherm for predicting the amount of diazinon adsorbed by Nano-PP/TiO_2. The hybrid fractional error function was developed to improve the fit of the sum square of errors at low concentrations. In this study, it ranged from 0.17 for the Freundlich model to 33.2 for the Temkin model. Also while evaluating MPSD, it was revealed that the Freundlich model

Table 3. Kinetic models parameters by linear regression method for the sorption of diazinon by nano-polypropylene-titanium dioxide composite

Kinetic models	Linear expression	Plot	Parameters	R^2	NSD	ARE	Parameters
Elovich	$q_t = \beta \ln(\alpha\beta) + \beta \ln t$	q_t vs. ln t	β=slope, α=(slope)$^{-1}$ exp(intercept/slope)	0.54	8.51	2.09	$\beta = -4.05$ g mg^{-1}; $\alpha = -0.92$ mg g^{-1} h^{-1}
Fractional power	ln q$_t$=lnk+v lnt	n q$_t$ vs. lnt	k=exp(intercept), v=slope	0.53	7.77	2.06	K=1.116 mg g^{-1} h^{-v}; v=-0.28
Zero order	$q_t = q_e - k_0 t$	q_t vs. t	q$_e$=intercept, k$_0$=$-$(slope)	0.82	4.81	1.29	K$_0$=0.007 mg g^{-1} h^{-1}; q$_m$=0.73 mg g^{-1}
First order	$\ln(q_e/q_t)=k_1 t$	ln(q$_t$) vs. t	q$_e$=exp(intercept), k$_{1p}$=$-$(slope)	0.81	4.89	1.34	K$_1$=0.016 h^{-1}; q$_m$=0.23 mg g^{-1}
Pseudo-first order	$\ln(q_e - q_t) = \ln q_e - k_{1p} t$	ln(q$_e$$-q_t$) vs. t	q$_e$=exp(intercept), k$_{1p}$=$-$(slope)	0.82	59.31	14.49	K$_{1p}$=-0.0028 h^{-1}; q$_m$=2.21 mg g^{-1}
Second order	$q_t^{-1} = q_e^{-1} + k_2 t$	q$_t^{-1}$ vs. t	q$_e$=(intercept)$^{-1}$, k$_2$=slope	0.81	59.76	16.89	K$_2$=0.0408 mg g^{-1} h^{-1}; q$_m$=0.98 mg g^{-1}
Pseudo-second order	Type(I) t/q$_t$ =1/k$_{2p}$q$_e^2$+t/q$_e$	t/q$_t$ vs. t	q$_e$=slope^{-1}, k$_{2p}$=(slope^2)/intercept	0.91	27.90	5.88	K$_{2p}$=0.483 mg g^{-1} h^{-1}; q$_m$=0.25 mg g^{-1}
	Type(II) 1/q$_t$ =(1/k$_{2p}$q$_e^2$)(1/t)+(1/q$_e$)	1/q$_t$ vs. 1/t	q$_e$=intercept^{-1}, k$_{2p}$=(intercept^2)/slope	0.34	59.37	16.71	K$_{2p}$=0.508 mg g^{-1} h^{-1}; q$_m$=0.344 mg g^{-1}
	Type(III) q$_t$ =q$_e$$-$(1/k$_{2p}q_e$)q$_t$/t	q$_t$ vs. q$_t$/t	q$_e$=intercept, k$_{2p}$=$-$1/(slope×intercept)	0.39	11.14	2.62	K$_{2p}$=-1.25 mg g^{-1} h^{-1}; q$_m$=0.408 mg g^{-1}
	Type(IV) q$_t$/t =k$_{2p}$q$_e^2$$-k_{2p}q_eq_t$	q/t vs. q$_t$	q$_e$=$-$intercept/slope, k$_{2p}$=(slope^2)/intercept	0.39	4,504.11	741.71	K$_{2p}$=-0.786 mg g^{-1} h^{-1}; q$_m$=254 mg g^{-1}
Intraparticle diffusion	$q_t = k_p t^{0.5}$	q$_t$ vs. t$^{0.5}$	k$_p$=slope	0.69	6.39	1.67	K$_{2p}$=-0.063 mg g^{-1} h$^{-0.5}$

had a minimum error. This function is similar to the geometric mean error distribution, which was modified according to the degree of freedom of the system. It has to be emphasized that the error obtained from MPSD and HYBRID seems essentially justified [37,38].

3. Kinetic Study

As shown in Table 3, the parameters and mechanism of kinetic adsorption of diazinon onto Nano-PP/TiO$_2$ were investigated by applying widely used models, including Elovich, fractional power, zero-order, first-order, second-order, pseudo-first-order, pseudo-second-order, and intra-particle diffusion [14,28,39].

Low correlation coefficients confirm that Elovich, fractional power, type II-IV of the linearized form of pseudo-second-order, and intra-particle diffusion kinetic models do not provide a better regression. Results suggest that the adsorption of diazinon onto Nano-PP/TiO$_2$ is most appropriately represented by a pseudo-second-order (type I) kinetic model because it has a higher R^2 than other models. This model assumes that two reactions either in series or in parallel are occurring; the first one is fast and reaches equilibrium quickly and the second is a slower reaction and can continue for a longer period [30].

As presented in Table 2, similar results were presented by other studies in adsorption of diazinon by various adsorbents including NH4Cl-induced activated carbon [29], alimentary industrial waste [31], and chitosan/carbon nanotube [16]. However, a different find-

ing was reported by using Mg-Al and Zn-Al layered double hydroxides adsorbent, which was consistent with the intra-particle diffusion kinetic model [36].

In addition, as presented in Eqs. (7) and (8), the applicability of the kinetic models was validated by the normalized standard deviation (NSD), and average relative error (ARE). Here, q_i^{Exp} is the experimental mass of diazinon adsorbed by Nano-PP/TiO$_2$, whereas q_i^{Cal} is calculated mass of diazinon adsorbed by Nano-PP/TiO$_2$. While N is the number of observations in the experimental isotherm [28].

$$\text{ARE} = \frac{100}{N} \sum_{i=1}^{N} \left| \frac{q_i^{Exp} - q_i^{Cal}}{q_i^{Exp}} \right| \tag{7}$$

$$\text{NSD} = 100 \sqrt{\left(\frac{1}{N-1} \sum_{i=1}^{N} \left[\frac{q_t^{Exp} - q_t^{Cal}}{q_t^{Exp}} \right]^2 \right)} \tag{8}$$

As presented in Table 3, for the consistent kinetic which was pseudo-second-order (R^2=0.91), the values of NSD and ARE were obtained as 27.90 and 5.88, respectively.

4. Optimization of Adsorption

Based on the central composite design (CCD), response surface methodology (RSM) was applied to design the experiments and survey the impact upon the factors on the adsorption efficiency. Table 4 exhibits the statistics of Linear, 2FI, Quadratic and cubic

Table 4. Statistics of different models used to optimize the adsorption of diazinon from water by nano-PP/TiO$_2$

Source	Std. Dev.	R-Squared	Adjusted R^2	Predicted R^2	PRESS	F-value	P-value
Linear	0.52	0.588	0.549	0.436	11.36	7.72	0.0001
2FI	0.44	0.731	0.676	0.602	8.42	6.01	0.0005
Quadratic	0.35	0.847	0.793	0.695	6.46	3.69	0.0148
Cubic	0.29	0.915	0.866	0.743	5.44	0.73	0.404

Table 5. Analysis of variance (ANOVA) for response surface quadratic model in adsorption of diazinon by nano-PP/TiO$_2$

Source	Sum of squares	Mean squares	F value	p-Value Prob>F
	Adsorption mg g^{-1}	Adsorption mg g^{-1}	Adsorption mg g^{-1}	Adsorption mg g^{-1}
Model	17.94	1.99	15.94	<0.0001
A- initial diazinon	7.71	7.71	61.64	<0.0001
B- adsorbent dose	5.66	5.66	45.25	<0.0001
C- Contact time	0.022	0.022	0.18	0.675
AB	3.03	3.03	24.24	<0.0001
AC	0.025	0.025	0.20	0.659
BC	0.0008	0.0008	0.007	0.934
A^2	0.67	0.67	5.34	0.029
B^2	2.08	2.08	16.67	0.0004
C^2	0.026	0.026	0.21	0.650
Residual lack of fit	1.52	0.3	3.69	0.0148
C.V., %	55.6			
PRESS	6.46			
R-squared	0.847			
Adjusted R^2	0.794			
Predicted R^2	0.695			
Adeq precision	14.95			

models which were used to select the most appropriate model for response surface factor in optimizing the adsorption of diazinon from water by Nano-PP/TiO$_2$. According to the output of Design-Expert software (version 7.0), the Quadratic model had the highest fit for studying the adsorption behavior of diazinon from water (F-value=3.69, P-value=0.0148). Therefore, the selected model was analyzed by using ANOVA within the Design-Expert software in the next step.

Table 5 provides information related to the analysis of variance for Quadratic model level response. Assessing ANOVA for Response Surface Quadratic Model in adsorption of diazinon by Nano-PP/TiO$_2$ demonstrated that the model F-value of 15.94 implies that the model is significant. The probability for the occurrence of "Model F-Value" due to noise is 0.01%. Values of "Prob>F" less than 0.05 indicate model terms are significant. In this case, A, B, AB, A^2, B^2 were significant model terms.

The "Pred R-Squared" of 0.695 is in reasonable agreement with the "Adj R-Squared" of 0.794. "Adeq Precision" measures the signal-to-noise ratio. A ratio greater than 4 is desirable. The ratio of 14.95 indicates an adequate signal. This model can be used to navigate the design space.

To create a model of the adsorption process, the final equation in terms of actual factors predicted the optimized state of adsorption of diazinon and was obtained according to Eq. (9). From this

equation, it can be concluded that adsorbent dose (factor B with a coefficient of 0.87) has the highest impact on the removal of diazinon from aqueous.

$$Adsorption(mg/g) = +0.625 + 0.173(A) - 0.879(B) - 0.006(C) - 0.02(AB)$$
$$+0.0014(AC) + 0.00015(BC) - 0.0032(A^2) + 0.185(B^2) + 0.00008(C2) \quad (9)$$

In Fig. 4(a), a normal probability plot of the studentized residuals checks for normality of residuals. Also, the plot of predicted adsorption versus actual adsorption (mg g^{-1}) is presented in Fig. 4(b).

Fig. 5 shows the impact of contact time and mass of adsorbent on the adsorption of diazinon by Nano-PP/TiO$_2$ in initial concentrations of 1 and 20 mg L^{-1}. By examining the slope of the related graphs, it appears that the rate of adsorption increases with increasing initial concentration of diazinon. The adsorption rate of diazinon was strongly related to the initial concentration of diazinon. The maximum adsorption rate was 0.4 mg g^{-1} in the initial concentration of 1 mg L^{-1} (Fig. 5(a)); while in the initial concentration of 20 mg L^{-1}, the rate of adsorption increased to 2.25 mg g^{-1} (Fig. 5(b)). In addition, Fig. 5 shows that the optimum contact time is a function of the initial concentration of diazinon and mass of adsorbent, while the initial amount of diazinon in water is high and the adsorbent mass is low. Whereas the rate of adsorption of diazinon by Nano-PP/TiO$_2$ reaches a maximum at minimum time. Consider that abundant target molecules are available in the high con-
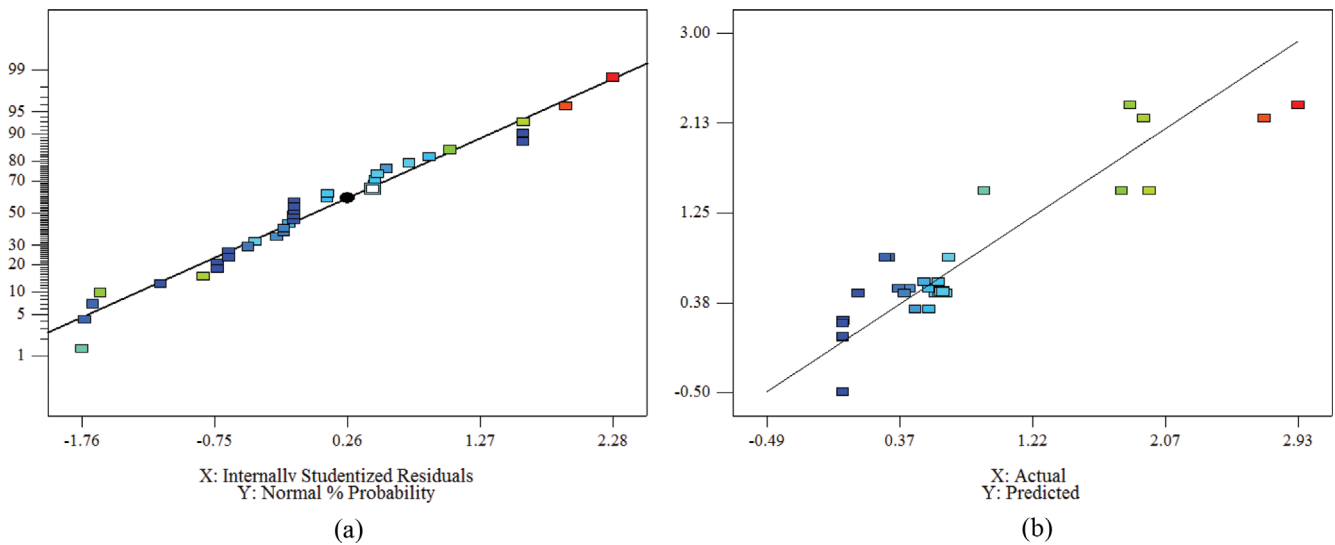
Fig. 4. (a) Normal probability plot of the studentized residuals and (b) plot of predicted vs. actual adsorption of Diazinon by Nano-PP/TiO$_2$.
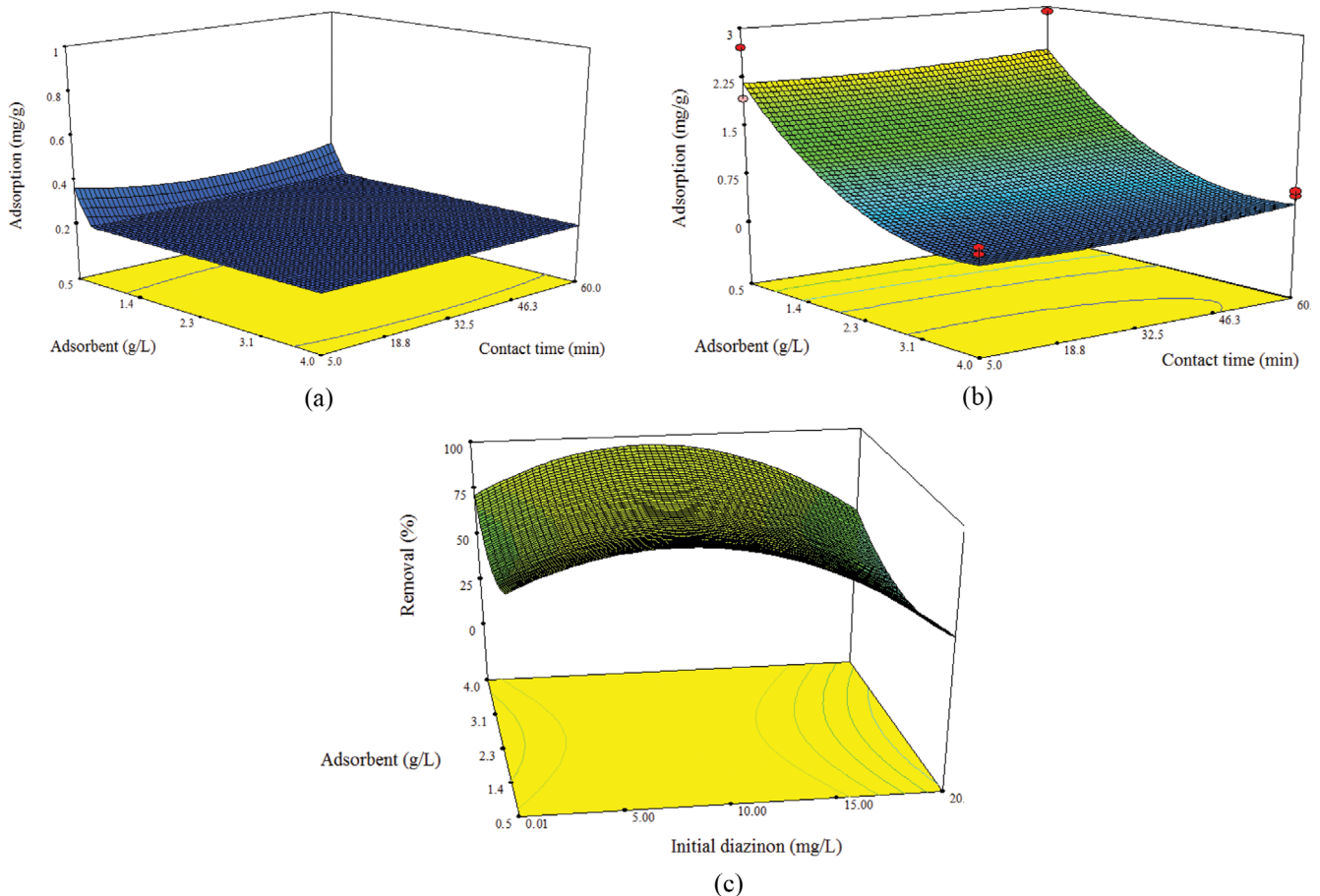

Fig. 5. Response surface graphs for adsorption of diazinon by Nano-PP/TiO$_2$ with interactions between contact time and adsorbent dose. (a) Initial concentration of 1 mg L^{-1}. (b) Initial concentration of 20 mg L^{-1}. (c) Trend of removal (%) in different initial concentration.

centration of diazinon on the surface center of Nano-PP/TiO$_2$ which increases mass transfer. Hence proving that the mass transfer had to be reinforced when the target molecules were accumulated at the interface of two phases of aqueous-adsorbent [32].

During the optimum conditions, the highest removal percent of the CCD method was equal to 69.3%. Results showed that a contact time of 32.2 min Nano-PP/TiO$_2$ with the dosage of 2.25 g L^{-1}, and initial diazinon concentration of 10 mg L^{-1} were achieved as
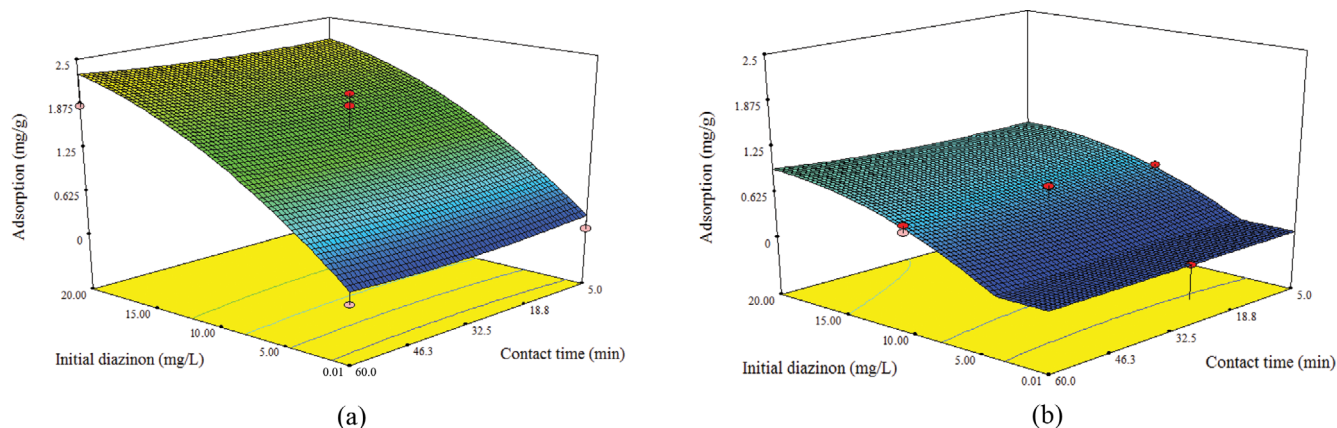
(a)   (b)

Fig. 6. Response surface graphs for adsorption of diazinon with interactions between contact time and initial diazinon concentration in different adsorbent dose of Nano-PP/TiO$_2$. (a) Adsorbent dose of 0.5 g L^{-1}. (b) Adsorbent dose of 2 g L^{-1}.

optimum conditions. Fig. 5(c) shows response surface graphs for the removal of diazinon from aqueous by Nano-PP/TiO$_2$. The removal percentage of diazinon by Nano-PP/TiO$_2$ was increased to 98% by increasing the initial concentration of diazinon from 0.5 to 10 mg L^{-1} and then a decline in the concentration was observed at the higher concentrations. At lower concentrations of diazinon, the specific surface area was high and more available to the diazinon molecules, but at concentrations higher than 10 mg L^{-1}, a decrease in the mass transfer occurred. Consequently, there was a lack of available unoccupied sites of Nano-PP/TiO$_2$. The same results were reported by Farhadi et al. [40]. which demonstrated that the removal of diazinon from water by Zero-valent iron supported on biopolymer chitosan was enhanced by increasing the initial concentration of diazinon from 10 to 100 mg L^{-1} [40].

Fig. 6 shows response surface graphs for adsorption of diazinon with interactions between contact time and initial concentration of diazinon in the different mass of Nano-PP/TiO$_2$. These graphs revealed that the maximum capacity of Nano-PP/TiO$_2$ occurs in the minimum mass of adsorbent. The maximum adsorption rate was 2.3 mg g^{-1} in the mass of 0.5 g L^{-1} (Fig. 6(a)); while with increasing adsorbent dose to 2 g L^{-1}, the adsorption decreased to lower than 0.9 mg g^{-1} (Fig. 6(b)). It shows that the optimum adsorbent dose of Nano-PP/TiO$_2$ is a function of the initial concentration of diazinon and contact time; while the initial amount of diazinon in water is high, and the contact time is low, the rate of adsorption of diazinon reaches a maximum at the minimum mass of Nano-PP/TiO$_2$. It indicates that by virtue of the rapid diazinon adsorption process through the adsorbent, the absorption time is short. Therefore, increasing the adsorbent mass does not affect the absorption rate.

CONCLUSION

The results of this study reveal that a smooth nanocomposite without bumps can be produced by coating polypropylene fibers with nano-titanium dioxide in wet heat under submerging in an ultrasonic chamber. The adsorption equilibrium and kinetic data were in better correspondence with Langmuir and pseudo-second-order reaction; that means the adsorption processes are well de-

scribed by two-stage diffusion. Results showed that the optimum condition occurred with the initial diazinon concentration=10 mg L^{-1}, contact time=32.2 min and mass of Nano-PP/TiO$_2$=2.25 g L^{-1} with the maximum removal efficiency of 69.3%. Based on the central composite design (CCD), response surface methodology (RSM) revealed that the adsorption capacity of diazinon by Nano-PP/TiO$_2$ was enhanced with the increase in adsorbent concentration, while removal per unit weight of adsorbent increased with the decrease in adsorbent concentration. Briefly, it can be concluded that Nano-PP/TiO$_2$ has a moderate adsorption affinity toward the organophosphate pesticides, making Nano-PP/TiO$_2$ a viable and efficient sorbent for the treatment of water and wastewater containing such contaminants.

AUTHOR CONTRIBUTIONS

Asma Barazandeh did experimental analysis. Hamzeh Ali Jamali helped in methodology and statistical analysis. Hamid Karyab did conceptualization and writing. In addition, all authors approved the final version of the manuscript and agreed to be accountable for all aspects of the study.

CONFLICT OF INTEREST

The authors declare that they have no conflict of interest.

REFERENCES

1. P. Gerber and B. Chen, *Altern. Law J.*, **36**, 1 (2011).
2. L. Liu, H. Ren, J. Wu, L. He, X. Wan and G. Yang, *Environ. Epidemiol.*, **3**, 246 (2019).
3. B. Said, F. Wright, G. Nichols, M. Reacher and M. Rutter, *Epidemiol. Infect.*, **130**, 3 (2003).
4. H. Karyab, A. H. Mahvi, S. Nazmara and A. Bahojb, *Environ. Con-*

tam Tox., **90**, 1 (2013).

5. M. Milhome, P. Sousa, F. Lima and R. Nascimento, *Int. J. Environ. Res.*, **9**, 1 (2015).

6. D. R. Smith, K. W. King, L. Johnson, W. Francesconi, P. Richards, D. Baker and A. N. Sharpley, *J. Environ. Qual.*, **44**, 2 (2015).

7. M. Sandin, K. Piikki, N. Jarvis, M. Larsbo, K. Bishop and J. Kreuger, *Sci. Total Environ.*, **610**, 623 (2018).

8. R. Dehghani, M. Shayeghi, H. Esalmi, S. G. Moosavi, D. K. Rabani and D. Hossein Shahi, Zahedan, *J. Res. Med. Sci.*, **14**, 10 (2012).

9. R. R. Kalantary, Y. Dadban Shahamat, M. Farzadkia, A. Esrafili and H. Asgharnia, *Desalin. Water Treat.*, **55**, 2 (2015).

10. G. Asgari, A. Seidmohammadi, A. Esrafili, J. Faradmal, M. N. Sepehr and M. Jafarinia, *RSC Adv.*, **10**, 13 (2020).

11. A. Maleki, F. Moradi, B. Shahmoradi, R. Rezaee and S. M. J. Lee, *J. Mol. Liq.*, **297**, 111918 (2020).

12. A. Amooey, A. Ghasemi, S. Mirsoleimani-azizi, S. M. Gholaminezhad and Z. M. J. Chaichi, *Korean J. Chem. Eng.*, **31**, 6 (2014).

13. S. Nikzad, A. A. Amooey and A. Alinejad-Mir, *Environ. Sci. Pollut. R.*, **28**, 16 (2021).

14. N. Sohrabi, R. Mohammadi, H. R. Ghassemzadeh and S. S. Heris, *J. Mol. Liq.*, **328**, 115384 (2021).

15. K. S. Ryoo, S. Y. Jung, H. Sim and J. H. Choi, *Korean Chem. Soc.*, **34**, 9 (2013).

16. T. T. Firozjaee, N. Mehrdadi, M. Baghdadi and G. Bidhendi, *Desalin. Water Treat.*, **79**, 291 (2017).

17. M. Ponnuchamy, A. Kapoor, P. S. Kumar, A. Balakrishnan, M. M. Jacob and P. Sivaraman, *Environ. Chem. Lett.*, **19**, 2425 (2021).

18. S. Chaudhari, T. Shaikh and P. Pandey, *Int. J. Eng. Res. Appl.*, **3**, 5 (2013).

19. M. M. Kamrannejad, A. Hasanzadeh, N. Nosoudi, L. Mai and A. A. Babaluo, *Mater. Res.*, **17**, 4 (2014).

20. M. Masoudifar, B. Nosrati and R. Mohebbi Gargari, *Int. Wood Prod. J.*, **9**, 4 (2018).

21. H. Karyab, F. Karyab and R. Haji-Mirmohammad Ali, *Desal. Water Treat.*, **98**, 144 (2017).

22. M. T. Islam, A. Dominguez, R. S. Turley, H. Kim, K. A. Sultana, M. Shuvo, B. Alvarado-Tenorio, M. O. Montes, Y. Lin and J. Gardea-Torresdey, *Sci. Total Environ.*, **704**, 135406 (2020).

23. N. Prorokova, T. Kumeeva and I. Kholodkov, *Coatings*, **10**, 1 (2020).

24. R. Szabová, Ľ. Černáková, M. Wolfová and M. Černák, *Acta Chim. Slov.*, **2**, 1 (2009).

25. A. Saleh, Y. Yamini, M. Faraji, M. Rezaee and M. Ghambarian, *J. Chromatogr. A*, **1216**, 39 (2009).

26. Y. Gao, Y. Masuda, W. S. Seo, H. Ohta and K. Koumoto, *Ceram. Int.*, **30**, 7 (2004).

27. C. Randorn, S. Wongnawa and P. Boonsin, *ScienceAsia*, **30**, 149 (2004).

28. A. Behnamfard and M. M. Salarirad, *J. Hazard. Mater.*, **170**, 1 (2009).

29. G. Moussavi, H. Hosseini and A. Alahabadi, *Chem. Eng. J.*, **214**, 172 (2013).

30. Z. B. Ouznadji, M. N. Sahmoune and N. Y. Mezenner, *Desalin. Water Treat.*, **57**, 4 (2016).

31. N. Y. Mezenner, H. Lagha, H. Kais and M. Trari, *App. Water Sci.*, **7**, 7 (2017).

32. S. De Gisi, G. Lofrano, M. Grassi and M. Notarnicola, *Sustainable Mater. Technologies*, **9**, 10 (2016).

33. N. Ayawei, A. N. Ebelegi and D. Wankasi, *J. Chem-NY*, **2017**, 3039817 (2017).

34. F.-C. Wu, B.-L. Liu, K. T. Wu and R.-L. Tseng, *Chem. Eng. J.*, **162**, 1 (2010).

35. A. Farmany, S. S. Mortazavi and H. Mahdavi, *J. Magn. Magn. Mater.*, **416**, 75 (2016).

36. A. Sohrabi, M. R. Yaftian, L. Dolatyari, M. S. S. Dorraji and P. Soheili-Azad, *J. Iran. Chem. Soc.*, **17**, 1411 (2020).

37. M. H. Dehghani, M. Faraji, A. Mohammadi and H. Kamani, *Korean J. Chem. Eng.*, **34**, 2 (2017).

38. C. S. Gulipalli, B. Prasad and K. L. Wasewar, *J. Eng. Sci. Technol.*, **6**, 5 (2011).

39. T. T. Firozjaee, N. Mehrdadi, M. Baghdadi and G. Bidhendi, *Desalin. Water Treat.*, **79**, 291 (2017).

40. S. Farhadi, M. R. Sohrabi, F. Motiee and M. Davallo, *J. Polym. Environ.*, **29**, 1 (2020).

41. M. Saeidi, A. Naeimi and M. Komeili, *Adv. Environ. Technol.*, **2**, 1 (2016).